NeuroImage: Clinical 2 (2013) 120–131

Contents lists available at ScienceDirect

NeuroImage: Clinical

journal homepage: www.elsevier.com/locate/ynicl

Regional cortical thickness in relapsing remitting multiple sclerosis: A multi-center study

Ponnada A. Narayana [a,*], Koushik A. Govindarajan [a], Priya Goel [a], Sushmita Datta [a], John A. Lincoln [b], Stacy S. Cofield [c], Gary R. Cutter [c], Fred D. Lublin [d], Jerry S. Wolinsky [b] and MRI Analysis Center at Houston; The CombiRx Investigators Group

[a] Department of Diagnostic and Interventional Imaging, University of Texas Medical School at Houston, 6431 Fannin, Houston, TX 77030, USA
[b] Department of Neurology, University of Texas Medical School at Houston, 6431 Fannin, Houston, TX 77030, USA
[c] Department of Biostatistics, University of Alabama at Birmingham, Birmingham, AL 35294, USA
[d] The Corinne Goldsmith Dickinson Center for Multiple Sclerosis, Mount Sinai School of Medicine, New York, NY 10029, USA

ARTICLE INFO

Article history:
Received 27 September 2012
Received in revised form 12 November 2012
Accepted 19 November 2012
Available online 30 November 2012

Keywords:
MRI
Multiple sclerosis
Cortical thickness
MS lesions
Segmentation

ABSTRACT

A comprehensive analysis of the global and regional values of cortical thickness based on 3D magnetic resonance images was performed on 250 relapsing remitting multiple sclerosis (MS) patients who participated in a multi-center, randomized, phase III clinical trial (the CombiRx Trial) and 125 normal controls. The MS cohort was characterized by relatively low clinical disability and short disease duration. An automatic pipeline was developed for identifying images with poor quality and artifacts. The global and regional cortical thicknesses were determined using FreeSurfer software. Our results indicate significant cortical thinning in multiple regions in the MS patient cohort relative to the controls. Both global cortical thinning and regional cortical thinning were more prominent in the left hemisphere relative to the right hemisphere. Modest correlation was observed between cortical thickness and clinical measures that included the extended disability status scale and disease duration. Modest correlation was also observed between cortical thickness and T1-hypointense and T2-hyperintense lesions. These correlations were very similar at 1.5 T and 3 T field strengths. A much weaker inverse correlation between cortical thickness and age was observed among the MS subjects compared to normal controls. This age-dependent correlation was also stronger in males than in females. The values of cortical thickness were very similar at 1.5 T and 3 T field strengths. However, the age-dependent changes in both global and regional cortical thicknesses were observed to be stronger at 3 T relative to 1.5 T.

1. Introduction

Cortical thinning on magnetic resonance imaging (MRI) is a consistent and early feature in multiple sclerosis (MS) brains (Sailer et al., 2003). Reduced mean cortical thickness, particularly in the frontal and temporal regions may be a predictor of epilepsy in relapsing remitting MS (RRMS) patients (Calabrese et al., 2012). In one of the earliest studies, Sailer et al. (2003) reported smaller average cortical thickness in MS patients compared to healthy controls and demonstrated that cortical thinning correlated with clinical disability and T1 hypointense (T1 lesions), and T2 hyperintense (T2 lesions) white matter (WM) lesion volumes. Chen et al. (2004), based on longitudinal study at two time points separated by one year, reported a correlation between the progression of disability and progression of MRI-detectable cortical pathology. In one of the largest studies, Charil et al. (2007) measured cortical thickness in 425 RRMS patients and reported a relation between cortical atrophy, WM lesion load, and disability. That investigation demonstrated regional patterns in cortical thinning that differed from normal aging and reported cortical atrophy even among patients with mild disability. Ramasamy et al. (2009) measured regional cortical thinning in 71 MS patients with different clinical phenotypes and reported more advanced cortical thinning in later stages of MS and reported a relation between cortical atrophy and neurologic disability. Calabrese et al. (2010) measured cortical thickness in 115 MS patients and reported cortical thinning to be diffuse and an early phenomenon. Cortical thinning was also observed to correlate with fatigue and cognitive deficits in MS (Calabrese et al., 2011).

While the above studies clearly demonstrated the presence of global cortical thinning in MS, regional changes were not always

* Corresponding author. Tel.: +1 713 500 7677; fax: +1 713 500 7684.
E-mail address: Ponnada.A.Narayana@uth.tmc.edu (P.A. Narayana).

2213-1582
http://dx.doi.org/10.1016/j.nicl.2012.11.009

consistent. This may reflect the relatively small number of subjects and/or inclusion of different phenotypes. For example, the studies by Sailer et al. (2003) included relatively small number of patients (11 RRMS and 9 secondary progressive MS). The study by Chen et al. (2004) also included relatively few patients (20 with stable and 10 with progressing disability). In addition, the 3D T1-weighted MRI used for measuring the cortical thickness were acquired with a relatively large slice thickness of 3 mm that would result in significant partial volume averaging and could compromise the accuracy of measured cortical thickness. In the study by Charil et al. (2007) which included a large number of patients, the slice thickness was also 3 mm. While not explicitly stated in their publication, the published figures suggest an average cortical thickness of >4.5 mm, a value much higher than the 3 mm previously reported by Zilles (1990). While Ramasamy et al. (2009) (71 MS and 17 clinically isolated syndrome patients) measured the cortical thickness, their main emphasis was on the atrophy of the deep gray matter (GM) structures. In addition, majority of these studies did not account for the gender and age effects on cortical thickness.

Except for the publication by Charil et al. (2007), all the studies mentioned above were single center studies. Multi-center studies of MS as currently implemented for phase 3 clinical trials require large sample sizes and usually include longitudinal disease monitoring by MRI. These studies provide a rich resource for developing and testing any MRI-based measure that might be considered as an advanced biomarker of the disease and as a potential measure of disease outcome. A potential disadvantage of multi-center studies is that the data usually are acquired on different scanners, operating at different field strengths and, with variable quality assurance (QA) program across different centers.

In order to evaluate some of the above limitations prior to embarking on a comprehensive longitudinal analysis, we measured cortical thickness in different brain regions in a subcohort of 250 RRMS subjects from MRI obtained at entry into a large, multicenter, randomized treatment trial and compared the results to 125 age- and gender-group matched normal controls. The MRI data on the trial subjects were acquired on different scanners (General Electric, Philips and Siemens) operating at 1.5 T or 3 T field strengths. We also investigated the relationship between the regional cortical thickness and other clinical and MRI measures including the extended disability status scale (EDSS), disease duration from symptom onset, and T2-hyperintense and T1 hypointense lesion volumes. Finally, we investigated the dependence of cortical thickness on age, gender, and magnetic field strength.

2. Material and methods

2.1. Patients

The 250 subjects included in this study were randomly chosen from 1008 subjects enrolled in the CombiRx Trial (NCT00211887). CombiRx was a 3-year, double-blind, multi-center randomized clinical trial sponsored by the National Institutes of Neurological Disorders and Stroke and focused on RRMS. The primary trial objective was to determine if a combination of interferon beta-1a and glatiramer acetate was more efficacious than either agent alone (Lindsey et al., 2012). Trial design and the demographic data on the entire trial cohort at baseline have been detailed (Lindsey et al., 2012). The demographic data along with the mean T1 and T2 lesion volumes on the 250 patient subcohort used in this study is summarized in Table 1.

2.2. MRI scans

The CombiRx Trial MRI protocol included the acquisition of 2D FLAIR, dual echo turbo spin echo (TSE) or fast spin echo (FSE) images, and pre- and post-contrast T1-weighted images (0.94 mm × 0.94 mm × 3 mm voxel dimension). 3D T1-weighted images (0.94 mm × 0.94 mm × 1.5 mm voxel dimension) were acquired either with spoiled gradient recalled echo (SPGR) or magnetization prepared rapid gradient echo (MPRAGE) sequences. For the sub-cohort evaluated in this study, images on 163 subjects were acquired at 1.5 T while images on the remaining 87 subjects were acquired at 3 T.

Table 1
Demographic data of subjects included in this study.

	Patients (250)	Controls (125)
Age (yrs ± SD, median, range)	38.2 ± 9, 37, 18–61	37.3 ± 10.8, 38, 20–59
Females (males)	188 (62)	92 (33)
Disease duration (yrs ± SD, median, range)	1.58 ± 3.06, 0.83, 0.04–24.8	NA
EDSS at baseline (mean ± SD, median, range)	1.85 ± 1.1, 2.0, 0–5	NA
T1 lesion volume in cc (mean ± SD, median, range)	1.78 ± 2.61, 0.78, 0.01–15.4	NA
T2 lesion volume in cc (mean ± SD, median, range)	10.11 ± 11.99, 5.07, 0.41–72.60	NA

2.3. Normal controls

125 age- and gender matched controls were included in this study. 3D T1-weighted image data on 60 normal controls at the single center (UT Houston) was acquired on a Philips 3 T scanner with MPRAGE with an isotropic resolution of 1 mm. To better simulate the heterogeneity of scanners used for the MS subcohort, we included 3D T1-weighted images on 65 normal controls (62 at 1.5 T and 3 at 3 T) from publicly available databases (http://www.oasis-brains.org; http://www.cma.mgh.harvard.edu/ibsr/data.html; http://ida.loni.ucla.edu). These images were resampled to an isotropic voxel size of 1 mm. The demographic data on the normal controls is included in Table 1.

2.4. MRI quality assurance

Despite efforts, poor image quality and protocol violations are not uncommon in multi-center MRI studies. In view of the large number of images acquired during each patient session, manual examination of all the images for QA is a formidable task. Therefore, we implemented and validated a pipeline that automatically identifies images with suboptimal quality and noncompliant protocol. The software reads the Digital Imaging and Communications in Medicine (DICOM) image header and flags images that are not MRI protocol compliant. It also identifies images with unacceptably low signal-to-noise ratio (SNR) and artifacts such as ghosting due to patient motion and aliasing. These flagged images were manually examined to determine whether to include them in the analysis. The performance of the pipeline was validated using images acquired on normal volunteers some of which were deliberately corrupted and in others the DICOM image headers were deliberately altered such that the scan parameters differed from those dictated by the protocol.

2.5. Cortical thickness measurements

Cortical thickness measurements were performed using the FreeSurfer pipeline as previously described (http://surfer.nmr.mgh.harvard.edu/fswiki, Dale et al., 1999; Fischl et al., 1999). All our analyses were performed using FreeSurfer v5.1.0 on a Linux platform. In brief, the pipeline has a volumetric and a surface-based stream. All image volumes were first registered to the template space and intensity normalized. The images were then skull-stripped based on a combination of the watershed algorithm and deformable template model (Ségonne et al., 2004). The output brain mask was then labeled using a probabilistic atlas.

The surface based stream consists of WM segmentation followed by tessellation that identifies GM and WM boundary and the pial

surface (Dale et al., 1999; Fischl et al., 1999). Likely WM voxels were identified using neighborhood intensity information. WM and pial surfaces were constructed after refining the initial surfaces generated for each hemisphere. Cortical thickness is defined by the FreeSurfer developers as "the average of the distance between the surface (pial) and the GM–WM boundary and the distance between the GM–WM boundary and the surface (pial)" (Fischl and Dale, 2000).

Geometric information derived from the cortical model and neuroanatomical conventions was used for complete labeling of the cortical gyri and sulci. In this study, we used the labels based on the Desikan–Killiany atlas for lobar cortical thickness measurements. Computation time for the FreeSurfer pipeline to generate surface maps and parcellated brain regions was about 15 h per subject.

2.6. Image segmentation

To investigate the relationship between regional cortical thickness and T2 and T1 lesion volumes, all images were segmented using MRIAP (magnetic resonance imaging automatic processing), an in-house developed processing pipeline. MRIAP is based on algorithms described elsewhere (Datta et al., 2006, 2007; Sajja et al., 2006). It was written in Interactive Data Language (IDL; Boulder, CO), and incorporates a number of preprocessing steps that include denoising using anisotropic diffusion filter (Perona and Malik, 1990), intensity inhomogeneity correction (SPM module, http://www.fil.ion.ucl.ac.uk/spm), intensity normalization (Nyul et al., 2000), and skull stripping (Datta et al., 2006). Images were segmented into cerebrospinal fluid (CSF), GM, WM, and T2 lesions (Sajja et al., 2006) based on dual echo FSE and FLAIR MRI. Briefly, following the image preprocessing, a two dimensional feature map was generated based on T2 and FLAIR images using the Parzen window classifier (Duda et al., 2001) as described by Bedell et al. (1997). This feature map was used to classify the whole brain into CSF, brain parenchyma, and lesions. Then the brain parenchyma was further segmented into GM and WM using the expectation maximization–hidden Markov random field (EM–HMRF) algorithm (Zhang et al., 2001). For minimizing the false lesion classifications, the contextual information was exploited. Finally, using the fuzzy-connectedness method (Udupa et al., 1997), the lesions were delineated. The T1 lesions were segmented using the gray scale morphological operations on the pre- and post-contrast T1-weighted images as described elsewhere (Datta et al., 2006).

2.7. Statistical analysis

Statistical difference maps (between MS and normal controls) were generated using the cortical thickness maps based on general linear model (GLM) analysis. The surface maps were smoothed as recommended by the developers using a kernel with a FWHM of 10 mm. A multiple comparison Monte Carlo simulation with 5000 iterations was used to make inferences at $p = 0.001$ with a false discovery rate of $p < 0.05$. Correlations between cortical thickness and T1 and T2 lesions and clinical scores were determined using Spearman correlation and the R and p values were determined. Student's *t*-test was used for evaluating the age differences between patients and controls and χ^2 test was used for gender differences.

3. Results

3.1. Subject data

Fig. 1 shows the age distribution of both MS patients and the group matched normal controls. There is no statistically significant difference in the age between MS and normal subjects ($p = 0.85$). The ratio of female to male is also not significantly different between these two groups ($p = 0.87$; χ^2 test). The histograms of EDSS, disease duration

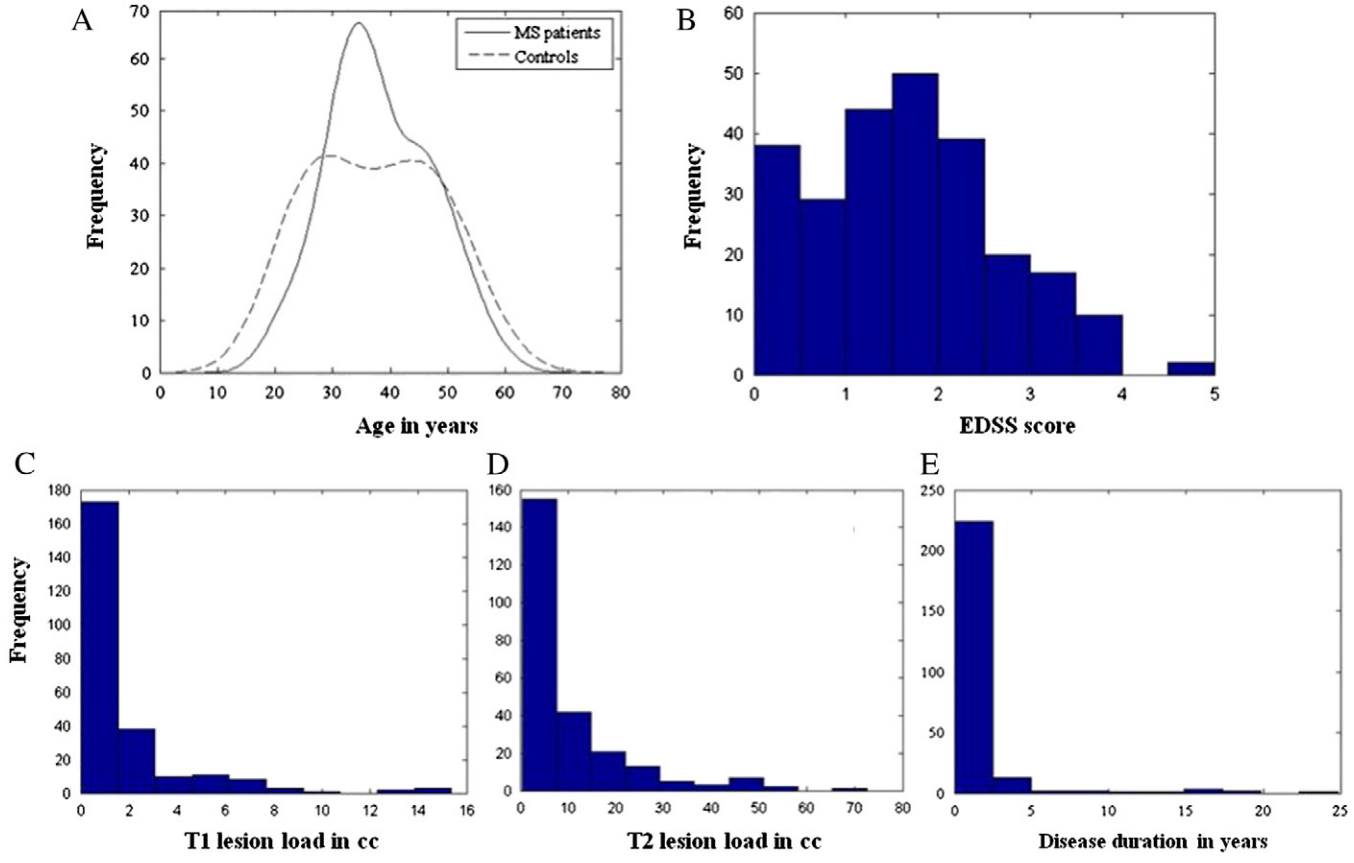

Fig. 1. Comparison of age distribution in MS patients and normal controls (A). Histograms of clinical parameters such as EDSS score (B), T1 lesion load (C), T2 lesion load (D) and disease duration (E) are also depicted.

and T1hypo- and T2 hyper-intense lesion volumes for characterizing the MS cohort included in this analysis are also shown in this figure.

3.2. Quality assurance

Twenty randomly selected images were deliberately corrupted to simulate either motion artifacts or aliasing or low SNR. Fig. 2 shows, as an example, two corrupted images: one with motion and the other with aliasing artifacts. This figure also shows images with poor SNR and ghosting artifacts. The software flagged all the corrupted images as being unacceptable. We also altered the image headers with scan parameters different from those prescribed in the protocol. The software flagged these images for protocol violation. In this study, we started with 264 actual MRI images; 14 were flagged for poor quality and/or protocol violation. All flagged images were inspected visually and were judged to be unacceptable for quantitative analysis. The final analysis was limited to the 250 image volumes that passed the QA tests.

3.3. Cortical thickness

Fig. 3 shows the regional cortical thinning in the left and right hemispheres in MS patients compared to age and gender matched controls. These images show the flattened (or inflated) brain. In this figure, different colors denote the multiple cortical regions with significant cortical thinning in the MS cohort relative to the controls. Table 2 summarizes the regions with significant cortical thinning. The extent of regional cortical thinning differed between the hemispheres. For example, the entorhinal cortex was more affected in the left compared to the right hemisphere. Similar observations were made in the pericalcarine cortex. Both these regions had the highest thinning in the left hemisphere. Overall, cortical thinning was more prominent in the left hemisphere relative to the right hemisphere.

3.4. Age and gender dependent changes in cortical thickness

The age dependent changes in the average cortical thickness over the whole brain in normal controls and MS subjects are shown in Fig. 4. These plots include both male and female subjects. The cortical thickness in healthy controls demonstrated relatively strong negative correlation with age. In contrast the average cortical thickness in MS patients showed only weak age dependence. Cortical thickness in MS patients was smaller than in normal controls at the corresponding age. In general, the regional structures showed stronger age dependence in healthy controls compared to MS patients. As an example, Fig. 5 shows the age dependent changes in the superior temporal lobe in MS subjects and healthy controls. The age dependent changes in regional cortical thickness are summarized in Table 3. Similar to that observed for mean cortical thickness, the cortical thicknesses for all the regions were smaller in the MS cohort than in the controls.

We investigated if gender confounded the age dependent changes in the cortical thickness. In general, males in the control population, showed stronger age related changes than females. This was also true among the MS patients. Fig. 6 shows the age dependent changes in mean cortical thickness in male and female MS subjects; males showed much stronger age related changes in cortical thickness compared to females. Similar gender associated changes were observed for all regional cortical structures that were investigated in this study. The results of correlation analysis are summarized in Table 4. It can be seen from this table that the normal controls show a stronger correlation than the MS subjects. Even though the sample size for males was only a third of that for females, the correlations were stronger among the males. Considering that our sample size in males was smaller than the females, we evaluated if the small sample size was the reason for stronger effects in males than in females. We applied the shrinkage factor (Yin and Fan, 2001) to the correlation coefficient and still found that the results showed stronger correlations in males than in females.

3.5. Magnetic field dependence of cortical thickness

Given the relatively small number of males available (36 males and 127 females at 1.5 T, and 26 males and 61 females at 3 T), we combined genders in this analysis. The mean cortical thickness for MS subjects at 3 T was 2.33 ± 0.19 mm, while at 1.5 T it was 2.38 ± 0.20 mm ($p = 0.051$); the corresponding values for normal controls were 2.41 ± 0.10 mm and 2.39 ± 0.09 mm ($p = 0.15$), respectively.

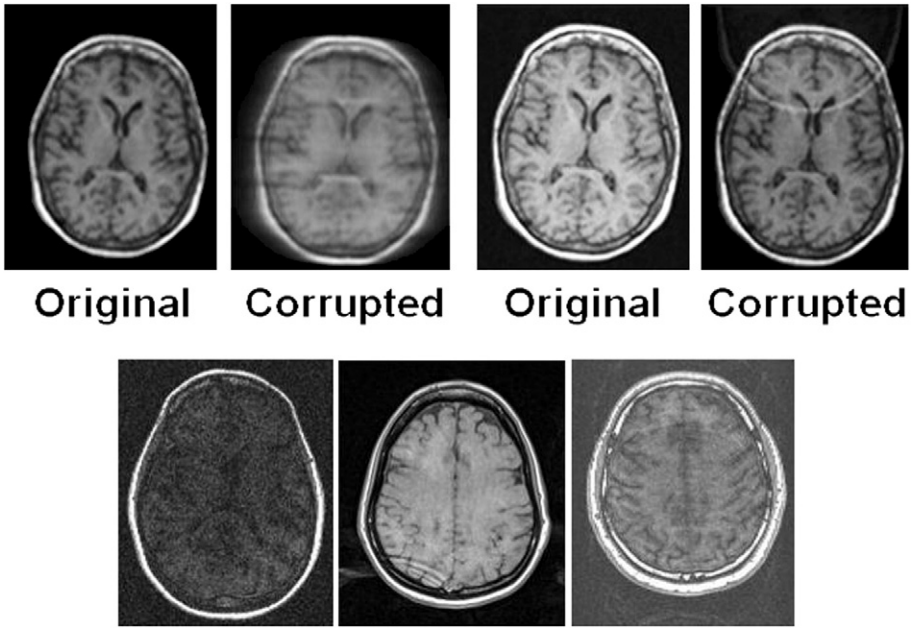

Fig. 2. Top panel: Original and deliberately corrupted images. The left panel shows a motion artifact and the right panel shows a fold-over artifact. Bottom panel: Corrupt images from the scanner discarded after QA protocol. The left image has poor SNR, the middle image shows a ringing artifact and the right image has a ghosting artifact.

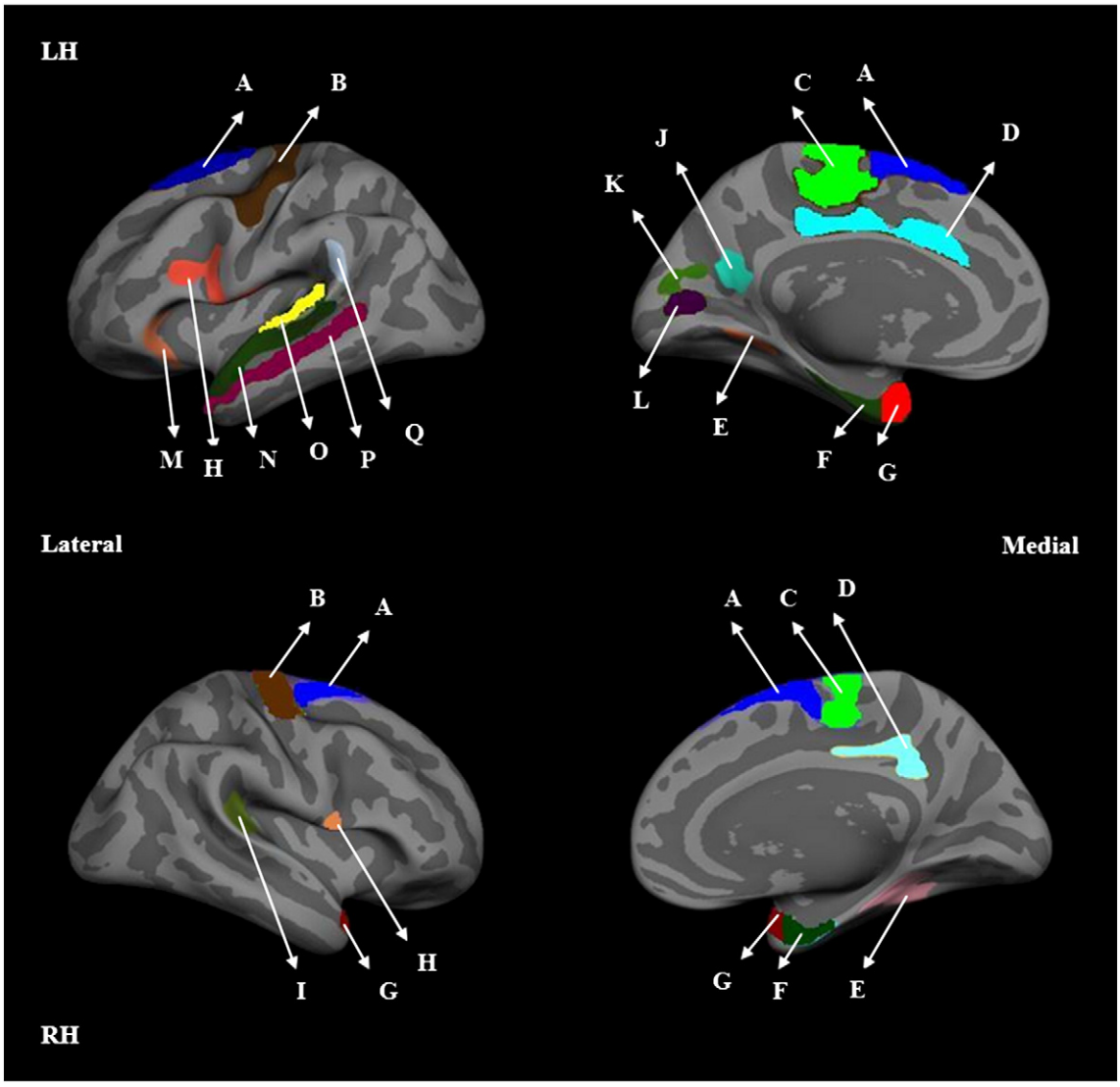

Fig. 3. Lateral (left column) and medial (right column) views of inflated left (LH; top row) and right (RH; bottom row) hemispheres. Images depict the group difference maps highlighting significantly thinner regions in 250 MS patients compared to 125 normal controls. The highlighted regions are: (A) superior frontal, (B) precentral, (C) paracentral, (D) cingulate, (E) fusiform, (F) entorhinal, (G) temporal pole, (H) pars opercularis, (I) transverse temporal, (J) precuneus, (K) cuneus, (L) pericalcerine, (M) pars orbitalis, (N) superior temporal, (O) transverse and parts of the superior temporal gyrus, (P) middle temporal and (Q) supramarginal.

Table 2
Regional cortical thinning in MS patients relative to normal controls. Only regions with significant thinning are included.

Structure	Left	Right
Banks of the superior temporal sulcus	5.57%	3.22%
Entorhinal	10.74%	7.94%
Fusiform	3.23%	2.55%
Parahippocampal	5.87%	6.21%
Paracentral	5.14%	2.93%
Precentral	5.97%	5.28%
Superior temporal	7.43%	5.14%
Temporal pole	9.39%	5.99%
Transverse temporal	6.52%	5.16%
Pericalcerine	3.89%	0.39%
Posterior cingulate	3.51%	1.92%
Pars opercularis	4.22%	3.15%
Middle temporal	3.87%	2.43%
Superior frontal	2.65%	2.21%
Pars orbitalis	0.96%	0.15%
Pars triangularis	2.29%	2.19%
Supramarginal	2.7%	2.92%
Precuneus	2.16%	2.4%
Cuneus	1.89%	0.92%
Lingual	1.36%	0.45%

3.6. Effect of magnetic field on age-dependent cortical thickness

The age dependence of cortical thickness in MS patients at 3 T was stronger ($R=-0.51$, $p=6.23e^{-7}$) than that seen at 1.5 T ($R=-0.1$, $p=0.2045$). For controls, the corresponding values were $R=-0.64$, $p=1.44e^{-8}$ at 3 T and $R=-0.31$, $p=0.015$ at 1.5 T. We also investigated the effect of field on the age dependent changes in regional cortical thickness in MS patients. The results are summarized in Table 5. As can be seen from this table, the trends were similar to the average cortical thicknesses. Similar field-dependent trends seen in MS patients were also observed in controls (data not shown).

3.7. Correlation between cortical thickness and lesion volumes

No significant correlations were found between the mean global cortical thickness and the T1 or T2 lesion volumes. Among all the regional structures investigated, one of the strongest, yet still modest, correlations seen were between T1 and T2 lesion volumes and superior temporal lobe cortical thickness (Fig. 7). Variable correlation

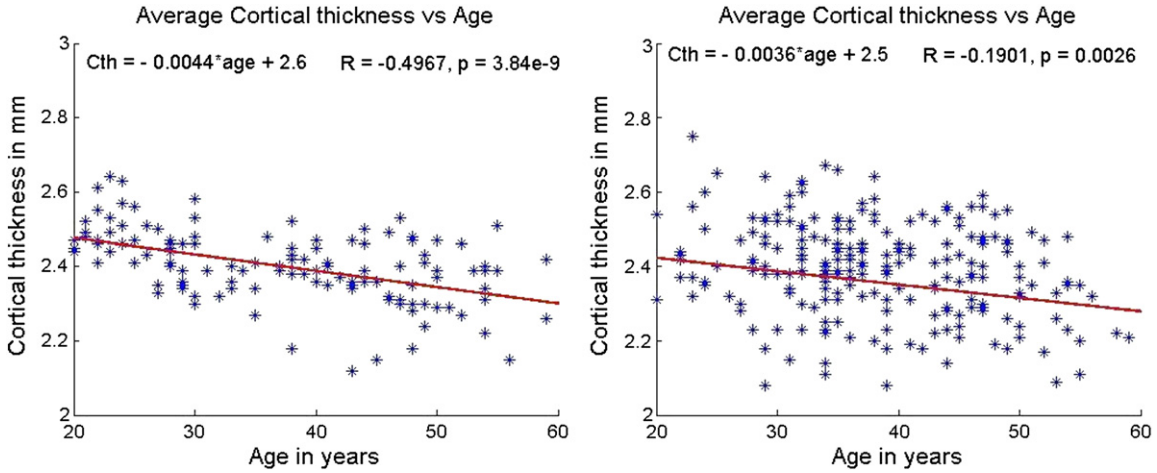

Fig. 4. Variation of whole brain cortical thickness with age in normal controls (left) and MS patients (right). The slope and intercept are reported on the top left corner and the R and p values based on Spearman correlation are on the top right corner. The scales have been matched for illustration purposes.

between lesion volumes and regional cortical thicknesses was observed. These results are summarized in Table 6.

3.8. Effect of magnetic field strength on correlation between cortical thickness and lesion volumes

Correlations between average cortical thickness and T1 and T2 lesion volumes were weak at both field strengths; at 1.5 T (T1 lesion volume: $R=-0.19$, $p=0.03$; T2 lesion volume: $R=-0.23$. $p=0.01$) and at 3 T (T1 lesion volume: $R=-0.14$, $p=0.21$; T2 lesion volume: $R=-0.1$, $p=0.4$). The observed correlations for regional thicknesses were very similar at both field strengths; 1.5 T (T1 lesion volume: range from $R=0$ to -0.32, T2 lesion volume: range $R=0$ to -0.39) and 3 T (T1 lesion volume: range $R=0$ to -0.27; T2 lesion volume: range $R=0$ to -0.33).

3.9. Correlation between cortical thickness and clinical variables

Only modest correlations were observed between cortical thickness (both average and regional) and EDSS, and no significant correlations were found with disease duration. As an example, Fig. 8 shows the variation of superior temporal cortical thickness with EDSS. The results of this analysis are summarized in Table 7. The temporal regions showed modest correlation with EDSS, but weak correlation with disease duration. The latter may be due to the limited spread in the disease duration in this patient cohort. The disease duration in the majority of these patients was within 3 years of onset of their first symptoms.

3.10. Effect of magnetic field strength on correlation between cortical thickness and clinical variables

The correlation between EDSS and average cortical thickness was not significant at either field strength: 1.5 T ($R=-0.02$, $p=0.86$) and 3 T ($R=-0.14$; $p=0.17$). The correlations between EDSS and regional cortical thickness were similar at both field strengths: 1.5 T (range $R=0$ to -0.19) and 3 T (range $R=0$ to -0.23). The correlations with both average and regional cortical thicknesses and disease duration at both field strengths were similar. The correlation between disease duration and average cortical thickness was not significant at either field strength: 1.5 T ($R=-0.06$, $p=0.42$) and 3 T ($R=-0.01$, $p=0.94$). The correlations between disease duration and regional cortical thickness were also similar at both field strengths with the exception of the right cingulate region at 3 T ($R=-0.3$, $p=0.002$). The correlations for the other regions were very weak at both field strengths: 1.5 T ($R=0$ to -0.18) and 3 T ($R=0$ to -0.23).

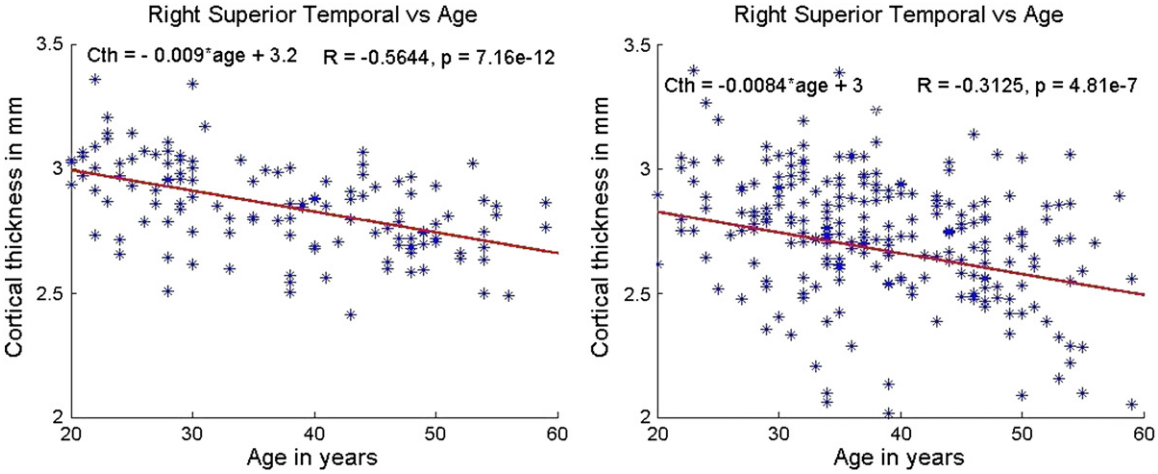

Fig. 5. Variation of superior temporal (right hemisphere) cortical thickness with age in normal controls (left) and MS patients (right). The slope and intercept are reported on the top left corner and the R and p values based on Spearman correlation are on the top right corner. The scales were matched for illustration purposes.

Table 3
Cortical thickness measurements of different regions correlated with age in 250 MS patients and 125 normal controls. R and p values are based on Spearman correlation.

Region	MS patients (N = 250)		Normal controls (N = 125)	
	Left hemisphere (R, p)	Right hemisphere (R, p)	Left hemisphere (R, p)	Right hemisphere (R, p)
Banks of the superior temporal sulcus	(-0.22, $4.94e^{-4}$)	(-0.26, $3.38e^{-5}$)	(-0.47, $2.2e^{-8}$)	(-0.37, $2.39e^{-5}$)
Entorhinal	(-0.14, 0.03)	(-0.06, 0.35)	(-0.16, 0.07)	(-0.23, 0.009)
Fusiform	(-0.26, $4.17e^{-5}$)	(-0.21, $7.4e^{-4}$)	(-0.49, $8.1e^{-9}$)	(-0.38, $1.41e^{-5}$)
Lingual	(-0.1, 0.13)	(-0.06, 0.36)	(-0.15, 0.1)	(-0.08, 0.4)
Middle temporal	(-0.26, $3.96e^{-5}$)	(-0.31, $6.08e^{-7}$)	(-0.52, $4.87e^{-10}$)	(-0.48, $1.39e^{-8}$)
Parahippocampal	(-0.17, 0.006)	(-0.01, 0.86)	(-0.41, $1.59e^{-6}$)	(-0.3, $7.31e^{-4}$)
Paracentral	(-0.12, 0.06)	(-0.17, 0.009)	(-0.26, 0.003)	(-0.31, $4.13e^{-4}$)
Pars opercularis	(-0.25, $7.45e^{-5}$)	(-0.32, $1.82e^{-7}$)	(-0.45, $1.63e^{-7}$)	(-0.43, $5.04e^{-7}$)
Pericalcerine	(-0.07, 0.26)	(-0.09, 0.17)	(0.07, 0.45)	(0.08, 0.37)
Posterior cingulate	(-0.24, $1.1e^{-4}$)	(-0.21, 0.001)	(-0.42, $1.35e^{-6}$)	(-0.25, 0.004)
Precentral	(-0.21, $9.32e^{-4}$)	(-0.18, 0.005)	(-0.34, $1.1e^{-4}$)	(-0.32, $2.31e^{-4}$)
Superior frontal	(-0.25, $6.95e^{-5}$)	(-0.29, $3.13e^{-6}$)	(-0.27, 0.002)	(-0.33, $1.97e^{-4}$)
Superior temporal	(-0.32, $1.74e^{-7}$)	(-0.31, $4.81e^{-7}$)	(-0.52, $5.26e^{-10}$)	(-0.56, $7.16e^{-12}$)
Temporal pole	(-0.10, 0.11)	(-0.17, 0.006)	(-0.33, $2.08e^{-4}$)	(-0.25, 0.005)
Transverse temporal	(-0.14, 0.03)	(-0.15, 0.02)	(-0.26, 0.003)	(-0.38, $1.26e^{-5}$)

4. Discussion

We investigated changes in global and regional cortical thicknesses in a relatively large and homogeneous cohort of 250 RRMS subjects with low clinical disability and short disease duration compared to a matched normal control group. The main contributions of this study include: implementation of automatic QA assessment of the MRI, investigation of changes in global and regional cortical thicknesses as a function of age, gender, and magnetic field strength, and correlation of cortical thinning with lesion volumes, EDSS, and disease duration.

The image artifacts and poor signal-to-noise ratio (SNR) affect the measured cortical thickness. Our automatic pipeline checked for image artifacts and SNR and flagged those images that were of inadequate quality. Thus in the current studies the effect of poor image quality on the cortical thickness measurements is minimized. To the best of our knowledge, this is the first study in which an automatic pipeline is implemented for QA in the analysis of large multi-center data.

It is pertinent to compare our results with the literature on cortical thinning in MS. Our studies, like those of Sailer et al. (2003), showed bilateral thinning of frontal and temporal association areas in RRMS subjects with mild clinical disability and/or short disease duration. Consistent with others (Calabrese et al., 2007), we demonstrated significant cortical thinning early in the disease, though, the reductions in cortical thickness in precentral and frontal areas were found to be smaller in our cohort. In contrast to the findings reported by Calabrese et al. (2007), we did not observe a significant reduction in cortical thickness in the occipital cortex, though various regions involving the medial surface of the occipital lobe, such as the pericalcarine, precuneus, and cuneus, were marginally affected. Ramasamy et al. (2009) reported reduced cortical thickness in multiple cortical regions that included the frontal pole, isthmus cingulate, caudal anterior cingulate, medial orbitofrontal and middle temporal in the left cerebral hemisphere and pars opercularis, supramarginal, inferior temporal and lateral orbitofrontal gyri in the right cerebral hemisphere. We observed reduced cortical thickness in similar cortical areas, and also in parahippocampal and lingual areas. The strongest reduction in cortical thickness was in the entorhinal cortex and temporal poles. Cortical thinning in these two neighboring structures has not been documented previously. The precentral gyrus is a region that consistently showed cortical thinning across all published studies.

Published correlations between cortical thickness and other MRI measures vary. Charil et al. (2007) reported highly significant correlation between global cortical thickness and the total WM lesion volumes. These authors also showed several cortical regions that included the bilateral cingulate gyri (mostly in the anterior part with Brodmann's area [BA] 32 and 24), and bilateral posterior insular cortex in the vicinity of the transverse temporal gyrus (BA 13 and 41)

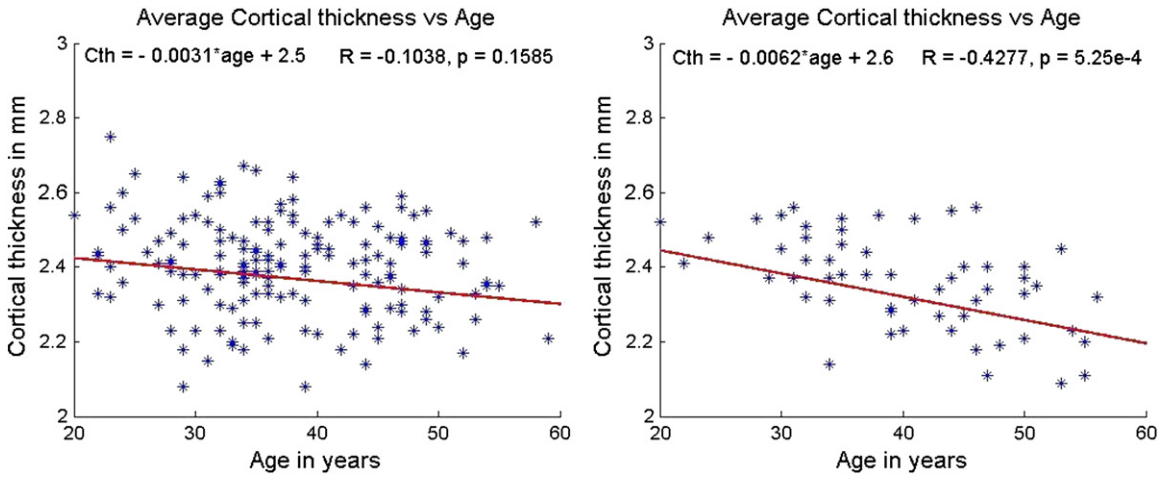

Fig. 6. Average cortical thickness as a function of age in MS patients (left — female, right — male). The slope and intercept are reported on the top left corner and the R and p values based on Spearman correlation are on the top right corner. The scales have been matched for illustration purposes.

Table 4
Cortical thickness measurements of different regions separated gender-wise correlated with age in 250 MS patients. R and p values from Spearman correlation are reported.

Region	Left hemisphere			
	MS patients (N = 250)		Normal controls (N = 125)	
	Males (N = 63) (R,p)	Females (N = 187) (R,p)	Males (N = 33) (R,p)	Females (N = 92) (R,p)
Banks of the superior temporal sulcus	(−0.27, 0.03)	(−0.1, 0.19)	(−0.49, 0.004)	(−0.28, 0.007)
Fusiform	(−0.29,0.02)	(−0.13, 0.07)	(−0.45, 0.009)	(−0.30, 0.004)
Inferior parietal	(−0.34, 0.007)	(−0.07, 0.31)	(−0.33, 0.06)	(−0.15, 0.15)
Inferior temporal	(−0.28, 0.026)	(−0.11, 0.14)	(−0.39, 0.02)	(−0.17, 0.10)
Lateral orbitofrontal	(−0.24, 0.06)	(−0.09, 0.23)	(−0.52, 0.002)	(−0.29, 0.005)
Middle temporal	(−0.31, 0.01)	(−0.14, 0.05)	(−0.44, 0.01)	(−0.32, 0.002)
Pars opercularis	(−0.42, $6.05e^{-04}$)	(−0.11, 0.15)	(−0.61, $1.90e^{-04}$)	(−0.31, 0.003)
Pars orbitalis	(−0.24, 0.06)	(−0.02, 0.81)	(−0.67, $2.03e^{-05}$)	(−0.32, 0.002)
Pars triangularis	(−0.25, 0.05)	(−0.09, 0.25)	(−0.36, 0.04)	(−0.32, 0.002)
Posterior cingulate	(−0.22, 0.08)	(−0.16, 0.03)	(−0.34, 0.05)	(−0.18, 0.08)
Precentral	(−0.33, 0.01)	(−0.09, 0.20)	(−0.34, 0.05)	(−0.20, 0.05)
Rostral middle frontal	(−0.24, 0.06)	(−0.02, 0.75)	(−0.56, $6.60e^{-04}$)	(−0.27, 0.009)
Superior temporal	(−0.42, $6.23e^{-04}$)	(−0.15, 0.04)	(−0.47, 0.006)	(−0.30, 0.004)
Supramarginal	(−0.39, 0.002)	(−0.12, 0.11)	(−0.54, 0.001)	(−0.26, 0.011)
Transverse temporal	(−0.27, 0.03)	(0.01, 0.89)	(−0.58, $4.32e^{-04}$)	(−0.12, 0.23)

that correlated with total lesion volume. However, we failed to observe a strong correlation between either global or regional cortical thickness and T1 and T2 lesion volumes. The strongest correlation we found was between the superior frontal region and both T1 and T2 lesion volumes. However, this was modest (about R = −0.3). This was true at both 1.5 T and 3 T. Similar to our observations, Calabrese et al. (2007) reported only modest correlation with T2 lesion volume (R = −0.393, p = 0.03). Our results suggest, consistent with earlier observations (Calabrese et al., 2007; Charil et al., 2007; De Stefano et al., 2003), that WM lesions only partly contribute to cortical atrophy.

We observed only modest correlation between global cortical thickness and EDSS at 1.5 T and 3 T field strengths. The correlation between EDSS and regional cortical thinning was either modest or not significant. Similarly, the maximum correlation between regional cortical thickness and the lesion volume was <0.3. Ramasamy et al. (2009) reported correlation between EDSS and the right parahippocampal (R = −0.409), left lateral occipital (R = −0.360), and left post central (R = −0.421) regions. This is somewhat different from the results we obtained in the current study. The correlation between global cortical thickness and disease duration was not significant at either field strength. This was also true for the regional cortical thickness, except for the right anterior and posterior cingulate cortices. At 3 T, a modest, but significant correlation (R = −0.3) was observed between the anterior and posterior cingulate and disease duration. The cingulate cortex is implicated in cognition and cognitive deficits in MS have been documented (Colorado et al., 2012; Filippi et al., 2012; Rocca et al., 2010).

There is a substantial literature on the age dependence of global and regional thicknesses in healthy controls. Consistent age related atrophy in regional cortical structures has been demonstrated (Abe et al., 2008; Dickerson et al., 2009; Fjell et al., 2009; Good et al., 2001; Lemaitre et al., 2012; Piguet et al., 2009; Raz et al., 2004; Tisserand et al., 2002, 2003; Ziegler et al., 2010). Perhaps in one of the largest studies, Fjell et al. (2009) investigated the age dependent cortical thickness in 883 controls drawn from six centers. These authors reported consistent age effects across subjects in the superior, middle, and inferior frontal gyri, superior and middle temporal gyri, precuneus, inferior and superior parietal cortices, fusiform and lingual gyri, and the temporo-parietal junction. The strongest effects were seen in the superior and inferior frontal gyri, as well as in the superior and middle temporal lobes, while moderate effects on age were seen in the medial-temporal cortices such as the parahippocampal and entorhinal regions. The inferior temporal lobe and anterior cingulate cortices are relatively less affected by age. Our results on only 125 normal controls are consistent with those reported by Fjell et al. (2009). In addition, Fjell et al. (2009) observed that regional cortical thicknesses varied linearly with age and they failed to detect any nonlinear variation. These results are also consistent with our own

Table 5
Correlation between age and regional cortical thickness in 250 MS patients at 1.5 T and 3 T. R and p values from Spearman correlation are included. Only those regions that showed significant dependence are included in this table.

Region	Left hemisphere		Right hemisphere	
	1.5 T (R, p)	3 T (R, p)	1.5 T (R, p)	3 T (R, p)
Banks of the superior temporal sulcus	(−0.07, 0.38)	(−0.21, 0.05)	(−0.17, 0.03)	(−0.47, $4.29e^{-6}$)
Entorhinal	(−0.04, 0.61)	(−0.27, 0.01)	(−0.09, 0.27)	(−0.29, $1.14e^{-3}$)
Fusiform	(−0.10, 0.20)	(−0.32, $2.74e^{-3}$)	(−0.18, 0.03)	(−0.41, $1.12e^{-4}$)
Inferior parietal	(−0.10, 0.19)	(−0.27, 0.01)	(−0.24, $2.3e^{-4}$)	(−0.39, $1.74e^{-4}$)
Inferior temporal	(−0.03, 0.75)	(−0.31, $4.12e^{-3}$)	(−0.09, 0.26)	(−0.40, $1.2e^{-4}$)
Middle temporal	(−0.07, 0.36)	(−0.36, $1.65e^{-3}$)	(−0.26, $9.33e^{-4}$)	(−0.43, $3.96e^{-5}$)
Pars opercularis	(0.05, 0.51)	(−0.29, 0.01)	(−0.22, 0.01)	(−0.55, $5.05e^{-8}$)
Pars orbitalis	(−0.01, 0.91)	(−0.28, 0.01)	(−0.19, 0.01)	(−0.40, $1.6e^{-4}$)
Pars triangularis	(0.03, 0.67)	(−0.29, 0.01)	(−0.22, $4.37e^{-3}$)	(−0.37, $4.27e^{-4}$)
Posterior cingulate	(−0.05, 0.56)	(−0.42, $4.79e^{-5}$)	(−0.14, 0.08)	(−0.43, $4.52e^{-5}$)
Precentral	(−0.07, 0.39)	(−0.25, 0.02)	(−0.12, 0.13)	(−0.37, $4.12e^{-4}$)
Precuneus	(−0.04, 0.62)	(−0.30, $4.6e^{-3}$)	(−0.22, $4.21e^{-3}$)	(−0.50, $7.84e^{-7}$)
Superior temporal	(−0.09, 0.24)	(−0.38, $3.45e^{-4}$)	(−0.25, $1.33e^{-3}$)	(−0.40, $3.23e^{-3}$)
Supramarginal	(−0.11, 0.17)	(−0.39, $2.28e^{-4}$)	(−0.22, 0.01)	(−0.43, $3.27e^{-5}$)
Transverse temporal	(−0.07, 0.38)	(−0.26, 0.02)	(−0.09, 0.27)	(−0.35, $9.41e^{-4}$)

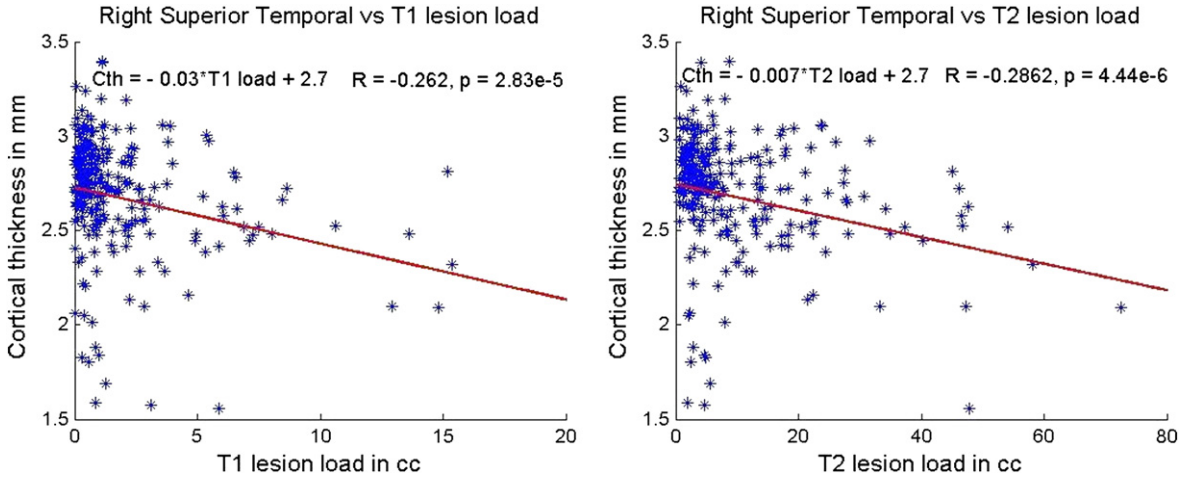

Fig. 7. Correlation between the right superior temporal cortex and T1 (left) and T2 (right) lesion loads. The slope and intercept are reported on the top left corner and the R and p values based on Spearman correlation are on the top right corner. The scales have been matched for illustration purposes.

studies. In contrast, Lemaitre et al. (2012) reported that the superior and inferior frontal, precentral and posterior cingulate cortical regions are the ones, which showed significant age-related atrophy. The cortical structures that showed relatively little age-dependence are the medial temporal lobe, including the entorhinal and parahippocampal cortices (Lemaitre et al., 2012; Salat et al., 2004). This is also consistent with our studies.

The age related changes in cortical thickness depend on the gender. However, the published literature on the impact of gender on cortical thickness is not always consistent. For example, Salat et al. (2004) reported that the age dependent changes in cortical thickness are very similar between males and females. In contrast, Sowell et al. (2007) reported that the age dependence of cortical thickness in men is significantly stronger than in women. Our results are consistent with those reported by Sowell et al. (2007).

We found weaker age dependent changes in both global and regional cortical thicknesses in MS patients compared to controls. The average cortical thickness correlated strongly with age ($R = -0.50$; $p = 3.84e^{-9}$) in normal controls. However, this correlation was only modest in MS patients ($R = -0.19$; $p = 0.003$). This differs from the value reported by Charil et al. (2007) who observed a correlation of 0.62 in MS patients. One potential explanation is that the ratio of females to males (197:228) in the study by Charil et al. (2007) was nearly equal while our MS cohort was made up of three times more females than males. Since the age dependence of global cortical thickness in men is significantly stronger than women, the age dependence is much weaker in our MS cohort. Moreover, the subjects studied by Charil et al. (2003) spanned a very broad range of EDSS disability. In contrast, our cohort is characterized by relatively low clinical disability and shorter disease duration. In addition, at age 20, the minimum age of our MS subjects, the mean cortical thickness is significantly smaller compared to normal controls at the corresponding age. Kochunov et al. (2011) observed the age dependent cortical thickness to be quadratic. However, both Salat et al. (2004) and we observed only a linear dependence. This is most probably due to the fact that Kochunov et al. (2011) included data from 1031 controls while our analysis was based on 125 normal controls, while Salat et al. (2004) included 106 subjects.

The pathology underlying reduced cortical thickness found on MRI in MS is not known. However, based on known histology of cortical lesions, it is tempting to postulate that demyelinating lesions may result in cortical thinning (Peterson et al., 2001; Vercellino et al., 2005). In a Marmoset model of experimental autoimmune encephalomyelitis (EAE) that replicates both gray- and white-matter lesions, Pomeroy et al. (2008) demonstrated that cortical thinning was not associated with focal demyelinating lesions. These authors postulated that cortical thinning was due to diffuse or more remote processes. Unfortunately, double inversion recovery (DIR) images, which are sensitive in

Table 6
Cortical thickness measurements of different regions correlated with T1 lesion load and T2 lesion load in 250 MS patients. R and p values from Spearman correlation are reported.

	MS patients (N = 250)		MS patients (N = 250)	
	Correlation with T1 lesion load		Correlation with T2 lesion load	
Region	Left hemisphere (R, p)	Right hemisphere (R, p)	Left hemisphere (R, p)	Right hemisphere (R, p)
Banks of the superior temporal sulcus	(−0.19, 0.002)	(-0.23, $2.38e^{-4}$)	(−0.17, 0.007)	(-0.23, $2.78e^{-4}$)
Entorhinal	(−0.15, 0.02)	(−0.05, 0.44)	(−0.1, 0.12)	(−0.06, 0.34)
Fusiform	(−0.17, 0.007)	(−0.15, 0.02)	(−0.16, 0.01)	(−0.14, 0.03)
Lingual	(−0.05, 0.42)	(−0.13, 0.04)	(−0.11, 0.08)	(−0.14, 0.03)
Middle temporal	(−0.16, 0.01)	(-0.24, $1.19e^{-4}$)	(−0.20, 0.001)	(-0.22, $4.26e^{-4}$)
Parahippocampal	(-0.21, $8.15e^{-4}$)	(−0.18, 0.005)	(−0.18, 0.004)	(−0.13, 0.05)
Paracentral	(−0.13, 0.04)	(−0.08, 0.18)	(−0.14, 0.03)	(−0.12, 0.06)
Pars opercularis	(-0.24, $1.78e^{-4}$)	(−0.2, 0.002)	(-0.25, $5.95e^{-5}$)	(−0.18, 0.005)
Pericalcerine	(−0.05, 0.46)	(−0.05, 0.44)	(−0.07, 0.30)	(−0.09, 0.13)
Posterior cingulate	(−0.17, 0.006)	(−0.20, 0.002)	(−0.13, 0.03)	(−0.14, 0.03)
Precentral	(−0.18, 0.005)	(−0.15, 0.02)	(-0.22, $3.74e^{-4}$)	(−0.15, 0.02)
Superior frontal	(-0.33, $1.48e^{-7}$)	(-0.35, $2.23e^{-8}$)	(-0.29, $3.13e^{-6}$)	(-0.3, $1.72e^{-6}$)
Superior temporal	(-0.23, $2.17e^{-4}$)	(-0.26, $2.83e^{-5}$)	(-0.28, $5.3e^{-6}$)	(-0.29, $4.44e^{-6}$)
Temporal pole	(-0.21, $6.75e^{-4}$)	(−0.19, 0.003)	(-0.22, $3.69e^{-4}$)	(−0.14, 0.03)
Transverse temporal	(−0.14, 0.03)	(−0.16, 0.01)	(−0.15, 0.02)	(−0.11, 0.09)

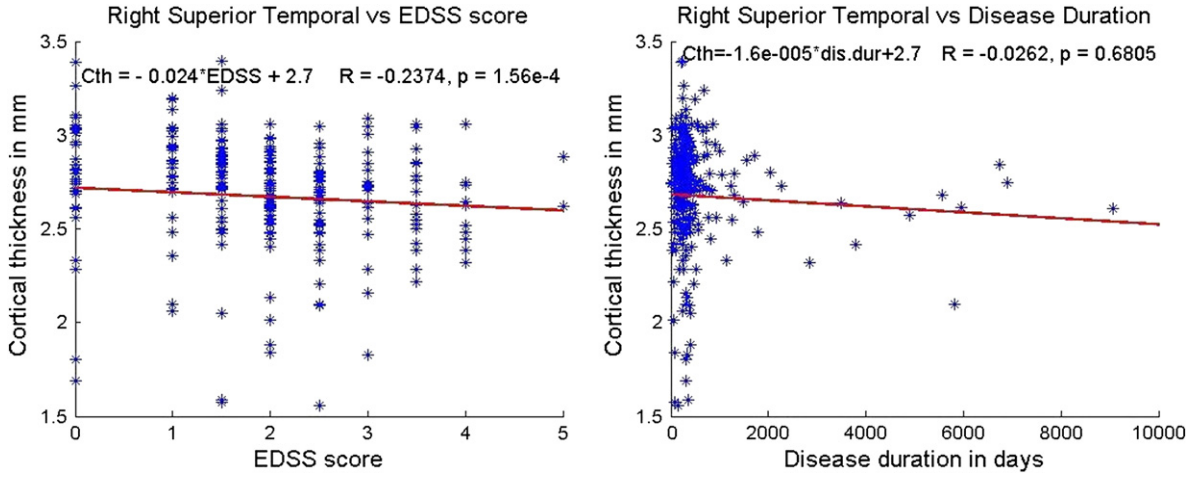

Fig. 8. Correlation between the right superior temporal cortex and EDSS score (left) and disease duration (right). The slope and intercept are reported on the top left corner and the R and p values based on Spearman correlation are on the top right corner. The scales have been matched for illustration purposes.

detecting cortical lesions (Geurts et al., 2005; Nelson et al., 2007) were not a part of the CombiRx MRI protocol. Thus, based on these studies, it is not possible to draw any conclusions about the association between cortical lesions and cortical atrophy.

We observed the left hemisphere to be more affected than the right hemisphere. Lemaitre et al. (2012) reported similar left–right asymmetry in multiple cortical structures in 216 healthy volunteers. Ramasamy et al. (2009) also showed more atrophy in majority of the deep gray matter structures in the left hemisphere compared to the right hemisphere. Our studies show that the left hemisphere, considered to be the dominant hemisphere, is more affected than the right. Perhaps this is related to the preponderance of right handed subjects (>85%) in our cohort.

We observed that both cortical thickness and its age dependence varied with magnetic field strength. In normal controls, the cortical thicknesses at 1.5 T and 3 T are not statistically different. Han et al. (2006) reported the mean cortical thickness to be slightly higher at 3 T relative to 1.5 T. However, these authors did not explicitly state whether the observed differences were statistically significant. In MS patients the cortex was slightly thicker at 1.5 T compared to 3 T, a difference, although not significant nearly reached significance at $p = 0.051$. The age related changes were observed to be stronger at 3 T compared to 1.5 T. This was true for both global and regional cortical thicknesses. The improved contrast-to-noise ratio at 3 T relative to 1.5 T might be a reason for these observed differences. These observations suggest that attention should be paid to the field strength at which MRI is acquired in interpreting the age dependent cortical thickness.

As described, the literature on global and regional cortical thicknesses in MS is not always consistent. The major reasons for the inconsistencies could be technical (image quality and spatial resolution), relatively small sample sizes, and inclusion of different MS phenotypes and heterogeneity within studied phenotypes. Our study differs from many of the published studies in a number of ways. Our sample size is relatively large and is restricted to a rather early and homogeneous RRMS clinical phenotype. By implementing an automatic pipeline, we addressed several issues related to image quality. Finally, our studies are very comprehensive and our analysis includes age, gender, and field dependence.

A shortcoming of the current study is that only cross sectional data were analyzed. While this is not as powerful as a longitudinal analysis, it was essential to demonstrate the feasibility of analyzing multi-center data acquired on different scanners and field strengths. Based on this feasibility study, we will move forward with a longitudinal analysis of the CombiRx Trial 3D MRI data and examine the predictive role of cortical thickness with clinical outcomes and its sensitivity to the different treatments applied in that trial. Additionally, our MS cohort represents subjects with relatively short disease

Table 7
Cortical thickness measurements of different regions correlated with EDSS scores and disease duration in 250 MS patients. R and p values from Spearman correlation are reported.

	MS patients (N = 250)		MS patients (N = 250)	
	Correlation with EDSS score		Correlation with disease duration	
Region	Left hemisphere (R, p)	Right hemisphere (R, p)	Left hemisphere (R, p)	Right hemisphere (R, p)
Banks of superior temporal sulcus	(−0.2, 0.002)	(−0.16, 0.01)	(−0.07, 0.26)	(−0.06, 0.39)
Entorhinal	(−0.04, 0.54)	(0.07, 0.26)	(0.04, 0.53)	(−0.03, 0.59)
Fusiform	(−0.12, 0.07)	(−0.1, 0.12)	(−0.02, 0.81)	(0.028, 0.66)
Lingual	(−0.21, 0.001)	(−0.15, 0.02)	(0.05, 0.43)	(0.09, 0.13)
Middle temporal	(−0.17, 0.008)	(−0.14, 0.03)	(−0.11, 0.07)	(−0.05, 0.42)
Parahippocampal	(−0.08, 0.23)	(−0.04, 0.5)	(−0.06, 0.32)	(−0.02, 0.74)
Paracentral	(−0.12, 0.05)	(−0.15, 0.02)	(−0.05, 0.42)	(−0.09, 0.17)
Pars opercularis	(−0.14, 0.03)	(−0.12, 0.05)	(−0.02, 0.7)	(−0.03, 0.67)
Pericalcerine	(−0.11, 0.07)	(−0.16, 0.01)	(0.05, 0.41)	(0.01, 0.85)
Posterior cingulate	(−0.05, 0.41)	(−0.07, 0.27)	(−0.06, 0.37)	(−0.06, 0.31)
Precentral	(−0.14, 0.03)	(−0.16, 0.01)	(−0.06, 0.36)	(−0.08, 0.22)
Superior frontal	(−0.09, 0.14)	(−0.12, 0.05)	(−0.07, 0.30)	(−0.07, 0.28)
Superior temporal	(−0.18, 0.004)	(−0.24, $1.56e^{-4}$)	(−0.12, 0.05)	(−0.05, 0.41)
Temporal pole	(−0.05, 0.41)	(−0.08, 0.21)	(−0.05, 0.47)	(−0.002, 0.97)
Transverse temporal	(−0.11, 0.09)	(−0.1, 0.12)	(−0.02, 0.79)	(−0.08, 0.21)

duration and low clinical disability. Thus, conclusions drawn about the correlations between cortical thickness and clinical measures might not generalize to more advanced disease states.

5. Conclusions

In this cross sectional study based on MRI, a comprehensive analysis of global and regional cortical thicknesses was performed on a relatively large and early RRMS cohort. An automatic pipeline for identifying images with suboptimal image quality and protocol violation is implemented as a part of the QA. In MS patients multiple cortical regions showed reduced cortical thickness compared to normal controls. Only a modest correlation between cortical thickness and T1 and T2 lesion volumes was observed both at 1.5 T and 3 T. Only a weak correlation was found between cortical thickness and EDSS or disease duration at either field strength. Age dependent changes in MS patients were observed to be weaker compared to normal controls. Both in normal and MS patients, the age dependent reductions in cortical thickness were weaker in females than in males. Finally, the field strength did not appear to affect the measured cortical thickness. However, the age dependent change in cortical thickness was observed to be stronger at 3 T relative to 1.5 T.

Acknowledgments

This work was supported by NINDS/NIH grant # R01NS078244. The CombiRx trial was supported by NINDS/NIH grant # U01 NS045719. Image segmentation was supported by NIBIB/NIH grant # 2 R01 EB02095. We would like to thank the OASIS (Open Access Series of Imaging Studies) database (Marcus et al., 2007; http://www.oasis-brains.org), the IBSR (Internet Brain Segmentation Repository) database (http://www.cma.mgh.harvard.edu/ibsr) and the ICBM (International Consortium of Brain Mapping) database (http://www.loni.ucla.edu/ICBM) for providing control subject data that was used in our analyses.

MRI Analysis Center

JS Wolinsky, PA Narayana, F Nelson, I Vainrub, S Datta, R He, B Gates, and K Ton.

The CombiRx Investigators Group

M. Agius, Sacramento, CA; K. Bashir, Birmingham, AL; R. Baumhefner, Los Angeles, CA; G. Birnbaum, Golden Valley, MN; G. Blevins, Edmonton, AB Canada; R. Bomprezzi, Phoenix, AZ; A. Boster, Columbus, OH; T. Brown, Kirkland, WA; J. Burkholder, Canton, OH; A. Camac, Lexington, MA; D. Campagnolo, Phoenix, AZ; J. Carter, Scottsdale, AZ; B. Cohen, Chicago, IL; J. Cooper, Berkeley, CA; J. Corboy, Aurora, CO; A. Cross, Saint Louis, MO; L. Dewitt, Salt Lake City, UT; J. Dunn, Kirkland, WA; K. Edwards, Latham, NY; E. Eggenberger, East Lansing, MI; J. English, Atlanta, GA; W. Felton, Richmond, VA; P. Fodor, Colorado Springs, CO; C. Ford, Albuquerque, NM; M. Freedman, Ottawa, Ontario, Canada; S. Galetta, Philadelphia, PA; G. Garmany, Boulder, CO; A. Goodman, Rochester, NY; M. Gottesman, Mineola, NY; C. Gottschalk, New Haven CT; M. Gruental, Albany, NY; M. Gudesblatt, Patchogue, NY; R. Hamill, Burlington, VT; J. Herbert, New York, NY; R. Holub, Albany, NY; W. Honeycutt, Maitland, FL; B. Hughes, Des Moines, IA; G. Hutton, Houston, TX; D. Jacobs, Philadelphia, PA; K. Johnson, Baltimore, MD; L. Kasper, Lebanon, NH; J. Kattah, Peoria, IL; M. Kaufman, Charlotte, NC; M. Keegan, Rochester, NY; O. Khan, Detroit, MI; B. Khatri, Milwaukee, WI; M. Kita, Seattle, WA; B. Koffman, Toledo, OH; E. Lallana, Lebanon, NH; N. Lava, Albany, NY; J. Lindsey, Houston, TX; P. Loge, Billings, MT; S. Lynch, Kansas City, KS; F. McGee, Richmond, VA; L. Mejico, Syracuse, NY; L. Metz, Calgary, AB Canada; P. O'Connor, Toronto, ON, Canada; K. Pandey, Albany, NY; H. Panitch, Burlington, VT; J. Preiningerova, New Haven, CT; K. Rammohan, Columbus, OH; C. Riley, New Haven, CT; P. Riskind, Worcester, MA; L. Rolak, Marshfield, WI; W. Royal, Baltimore, MD; S. Scarberry, Fargo, ND; A. Schulman, Richmond, VA; T. Scott, Pittsburgh, PA; C. Sheppard, Uniontown, OH; W. Sheremata, Miami, FL; L. Stone, Cleveland, OH; W. Stuart, Atlanta, GA; S. Subramaniam, Nashville, TN; V. Thadani, Lebanon, NH; F. Thomas, Saint Louis, MO; B. Thrower, Atlanta, GA; M. Tullman, New York, NY; A. Turel, Danville, PA; T. Vollmer, Phoenix, AZ; S. Waldman, La Habra, CA; B. Weinstock-Guttman, Buffalo, NY; J. Wendt, Tucson, AZ; R. Williams, Billings, MT; D. Wynn, Northbrook, IL; M. Yeung, Calgary, AB Canada.

References

Abe, O., Yamasue, H., Aoki, S., Suga, M., Yamada, H., Kasai, K., Masutani, Y., Kato, N., Ohtomo, K., 2008. Aging in the CNS: comparison of gray/white matter volume and diffusion tensor data. Neurobiology of Aging 29, 102–116.

Bedell, B.J., Narayana, P.A., Wolinsky, J.S., 1997. A dual approach for minimizing false lesion classifications on magnetic resonance images. Magnetic Resonance in Medicine 37, 94–102.

Calabrese, M., Atzori, M., Bernardi, V., Morra, A., Romualdi, C., Rinaldi, L., McAuliffe, M.J., Barachino, L., Perini, P., Fischl, B., Battistin, L., Gallo, P., 2007. Cortical atrophy is relevant in multiple sclerosis at clinical onset. Journal of Neurology 254, 1212–1220.

Calabrese, M., Rinaldi, F., Mattisi, I., Grossi, P., Favaretto, A., Atzori, M., Bernardi, V., Barachino, L., Romualdi, C., Rinaldi, L., Perini, P., Gallo, P., 2010. Widespread cortical thinning characterizes patients with MS with mild cognitive impairment. Neurology 74, 321–328.

Calabrese, M., Rinaldi, F., Grossi, P., Gallo, P., 2011. Cortical pathology and cognitive impairment in multiple sclerosis. Expert Review of Neurotherapeutics 11 (3), 425–432.

Calabrese, M., Grossi, P., Favaretto, A., Romualdi, C., Atzori, M., Rinaldi, F., Perini, P., Saladini, M., Gallo, P., 2012. Cortical pathology in multiple sclerosis patients with epilepsy: a 3 year longitudinal study. Journal of Neurology, Neurosurgery, and Psychiatry 83, 49–54.

Charil, A., Zijdenbos, A.P., Taylor, J., Boelman, C., Worsley, K.J., Evans, A.C., et al., 2003. Statistical mapping analysis of lesion location and neurological disability in multiple sclerosis: application to 452 patient data sets. NeuroImage 19, 532–544.

Charil, A., Dagher, A., Lerch, J.P., Zijdenbos, A.P., Worsley, K.J., Evans, A.C., 2007. Focal cortical atrophy in multiple sclerosis: relation to lesion load and disability. NeuroImage 34, 509–517.

Chen, J.T., Narayanan, S., Collins, D.L., Smith, S.M., Matthews, P.M., Arnold, D.L., 2004. Relating neocortical pathology to disability progression in multiple sclerosis using MRI. NeuroImage 23, 1168–1175.

Colorado, R.A., Shukla, K., Zhou, Y., Wolinsky, J.S., Narayana, P.A., 2012. Multi-task functional MRI in multiple sclerosis patients without clinical disability. NeuroImage 59, 573–581.

Dale, A.M., Fischl, B., Sereno, M.I., 1999. Cortical surface-based analysis. I. Segmentation and surface reconstruction. NeuroImage 9, 179–194.

Datta, S., Sajja, B.R., He, R., Wolinsky, J.S., Gupta, R.K., Narayana, P.A., 2006. Segmentation and quantification of black holes in multiple sclerosis. NeuroImage 29, 467–474.

Datta, S., Sajja, B.R., He, R., Gupta, R.K., Wolinsky, J.S., Narayana, P.A., 2007. Segmentation of gadolinium-enhanced lesions on MRI in multiple sclerosis. Journal of Magnetic Resonance Imaging 25, 932–937.

De Stefano, N., Matthews, P.M., Filippi, M., Agosta, F., De Luca, M., Bartolozzi, M.L., Guidi, L., Ghezzi, A., Montanari, E., Cifelli, A., Federico, A., Smith, S.M., 2003. Evidence of early cortical atrophy in MS: relevance to white matter changes and disability. Neurology 60, 1157–1162.

Dickerson, B.C., Feczko, E., Augustinack, J.C., Pacheco, J., Morris, J.C., Fischl, B., Buckner, R.L., 2009. Differential effects of aging and Alzheimer's disease on medial temporal lobe cortical thickness and surface area. Neurobiology of Aging 30, 432–440.

Duda, R.O., Hart, P.E., Stork, D.G., 2001. Pattern Classification. John Wiley & Sons, New York.

Filippi, M., Riccitelli, G., Mattioli, F., Capra, R., Stampatori, C., Pagani, E., Valsasina, P., Copetti, M., Falini, A., Comi, G., Rocca, M.A., 2012. Multiple sclerosis: effects of cognitive rehabilitation on structural and functional MR imaging measures—an explorative study. Radiology 262, 932–940.

Fischl, B., Dale, A.M., 2000. Measuring the thickness of the human cerebral cortex from magnetic resonance images. Proceedings of the National Academy of Sciences of the United States of America 97, 11050–11055 Sep.

Fischl, B., Sereno, M.I., Dale, A.M., 1999. Cortical surface-based analysis. II: inflation, flattening, and a surface-based coordinate system. NeuroImage 9, 195–207.

Fjell, A.M., Westlye, L.T., Amlien, I., Espeseth, T., Reinvang, I, Raz, N., Agartz, I., Salat, D.H., Greve, D.N., Fischl, B., Dale, A.M., Walhovd, K.B., 2009. High consistency of regional cortical thinning in aging across multiple samples. Cerebral Cortex 19, 2001–2012.

Geurts, J.J.G., Pouwels, P.J., Uitdehaag, B.M., Polman, C.H., Barkhof, F., Castelijns, J.A., 2005. Intracortical lesions in multiple sclerosis: improved detection with 3D double inversion recovery MR imaging. Radiology 236, 254–260.

Good, C.D., Johnsrude, I.S., Ashburner, J., Henson, R.N., Friston, K.J., Frackowiak, R.S., 2001. A voxel-based morphometric study of ageing in 465 normal adult human brains. NeuroImage 14, 21–36.

Han, X., Jovicich, J., Salat, D., van der Kouwe, A., Quinn, B., Czanner, S., Busa, E., Pacheco, J., Albert, M., Killiany, R., Maguire, P., Rosas, D., Makris, N., Dale, A., Dickerson, B., Fischl, B., 2006. Reliability of MRI-derived measurements of human cerebral cortical thickness: the effects of field strength, scanner upgrade and manufacturer. NeuroImage 32, 180–194.

Kochunov, P., Glahn, D.C., Lancaster, J., Thompson, P.M., Kochunov, V., Rogers, B., Fox, P., Blangero, J., Williamson, D.E., 2011. Fractional anisotropy of cerebral white matter and thickness of cortical gray matter across the lifespan. NeuroImage 58, 41–49.

Lemaitre, H., Goldman, A.L., Sambataro, F., Verchinski, B.A., Meyer-Lindenberg, A., Weinberger, D.R., Mattay, V.S., 2012. Normal age-related brain morphometric changes: nonuniformity across cortical thickness, surface area and gray matter volume? Neurobiology of Aging 33 (617), e1–e9.

Lindsey, J.W., Scott, T.F., Lynch, S.G., Cofield, S.S., Nelson, F., Conwit, R., et al., 2012. The CombiRx trial of combined therapy with interferon and glatiramer acetate in relapsing remitting MS: design and baseline characteristics. Multiple Sclerosis and Related Disorders 1, 81–86.

Marcus, D.S., Wang, T.H., Parker, J.M., Csernansky, J.G., Morris, J.C., Buckner, R.L., 2007. Open Access Series of Imaging Studies (OASIS): cross-sectional MRI data in young, middle aged, nondemented and demented older adults. Journal of Cognitive Neuroscience 19, 1498–1507.

Nelson, F., Poonawalla, A.H., Hou, P., Huang, F., Wolinsky, J.S., Narayana, P.A., 2007. Improved identification of intracortical lesions in multiple sclerosis with phase-sensitive inversion recovery in combination with fast double inversion recovery MR imaging. AJNR. American Journal of Neuroradiology 28, 1645–1649.

Nyul, L.G., Udupa, J.K., Zhang, X., 2000. New variants of a method of MRI scale standardization. IEEE Transactions on Medical Imaging 19, 143–150.

Perona, P., Malik, J., 1990. Scale-space and edge detection using anisotropic diffusion. IEEE Transactions on Pattern Analysis and Machine Intelligence 12, 629–639.

Peterson, J., Bo, L., Mork, S., Chang, A., Trapp, B., 2001. Transected neurites, apoptotic neurons, and reduced inflammation in cortical multiple sclerosis lesions. Annals of Neurology 50, 389–400.

Piguet, O., Double, K.L., Kril, J.J., Harasty, J., Macdonald, V., McRitchie, D.A., Halliday, G.M., 2009. White matter loss in healthy ageing: a postmortem analysis. Neurobiol Aging 30, 1288–1295.

Pomeroy, I.M., Jordan, E.K., Frank, J.A., Matthews, P.M., Esiri, M.M., 2008. Diffuse cortical atrophy in a marmoset model of multiple sclerosis. Neuroscience Letters 437, 121–124.

Ramasamy, D.P., Benedict, R.H., Cox, J.L., Fritz, D., Abdelrahman, N., Hussein, S., Minagar, A., Dwyer, M.G., Zivadinov, R., 2009. Extent of cerebellum, subcortical and cortical atrophy in patients with MS: a case–control study. Journal of the Neurological Sciences 282, 47–54.

Raz, N., Gunning-Dixon, F., Head, D., Rodrigue, K.M., Williamson, A., Acker, J.D., 2004. Aging, sexual dimorphism, and hemispheric asymmetry of the cerebral cortex: replicability of regional differences in volume. Neurobiology of Aging 25, 377–396.

Rocca, M.A., Valsasina, P., Absinta, M., Riccitelli, G., Rodegher, M.E., Misci, P., Rossi, P., Falini, A., Comi, G., Filippi, M., 2010. Default-mode network dysfunction and cognitive impairment in progressive MS. Neurology 74, 1252–1259.

Sailer, M., Fischl, B., Salat, D., Tempelmann, C., Schönfeld, M.A., Busa, E., Bodammer, N., Heinze, H.J., Dale, A., 2003. Focal thinning of the cerebral cortex in multiple sclerosis. Brain 126, 1734–1744.

Sajja, B.R., Datta, S., He, R., Mehta, M., Gupta, R.K., Wolinsky, J.S., Narayana, P.A., 2006. Unified approach for multiple sclerosis lesion segmentation on brain MRI. Annals of Biomedical Engineering 34, 142–151.

Salat, D.H., Buckner, R.L., Snyder, A.Z., Greve, D.N., Desikan, R.S., Busa, E., Morris, J.C., Dale, A.M., Fischl, B., 2004. Thinning of the cerebral cortex in aging. Cerebral Cortex 14, 721–730.

Ségonne, F., Dale, A.M., Busa, E., Glessner, M., Salat, D., Hahn, H.K., Fischl, B., 2004. A hybrid approach to the skull stripping problem in MRI. NeuroImage 22, 1060–1075.

Sowell, E.R., Peterson, B.S., Kan, E., Woods, R.P., Yoshii, J., Bansal, R., Xu, D., Zhu, H., Thompson, P.M., Toga, A.W., 2007. Sex differences in cortical thickness mapped in 176 healthy individuals between 7 and 87 years of age. Cerebral Cortex 17, 1550–1560.

Tisserand, D.J., Pruessner, J.C., Sanz Arigita, E.J., van Boxte, lMP, Evans, A.C., Jolles, J., Uylings, H.B., 2002. Regional frontal cortical volumes decrease differentially in aging: an MRI study to compare volumetric approaches and voxel-based morphometry. NeuroImage 17, 657–669.

Udupa, J.K., Wei, L., Samarasekera, S., Miki, Y., van Buchem, M.A., Grossman, R.I., 1997. Multiple sclerosis lesion quantitation using fuzzy-connectedness principles. IEEE Transactions on Medical Imaging 16, 598–609.

Vercellino, M., Plano, F., Votta, B., Mutani, R., Giordana, M.T., Cavalla, P., 2005. Grey matter pathology in multiple sclerosis. Journal of Neuropathology and Experimental Neurology 64, 1101–1107.

Yin, P., Fan, X., 2001. Estimating R^2 shrinkage in multiple regression: a comparison of different analytical methods. The Journal of Experimental Education 69 (2), 203–224.

Zhang, Y., Brady, M., Smith, S., 2001. Segmentation of brain MR images through a hidden Markov random field model and the expectation-maximization. IEEE Transactions on Medical Imaging 20, 45–57.

Ziegler, D.A., Piguet, O., Salat, D.H., Prince, K., Connally, E., Corkin, S., 2010. Cognition in healthy aging is related to regional white matter integrity, but not cortical thickness. Neurobiology of Aging 31, 1912–1926.

Zilles, K., 1990. The Human Nervous System. Academic Press, San Diego, CA.